EUROGRAPHICS '97 / D. Fellner and L. Szirmay-Kalos
(Guest Editors)

Volume 16, (1997), Number 3

Computing Volumes of Solids Enclosed by Recursive Subdivision Surfaces

Jörg Peters † and Ahmad Nasri ‡

Abstract

The volume of a solid enclosed by a recursive subdivision surface can be approximated based on the closed-form representation of regular parts of the subdivision surface and a tight estimate of the local convex hull near extraordinary points. The approach presented is efficient, i.e. non-exponential, and robust in that it yields rapidly contracting error bounding boxes. An extension to measuring higher-order moments is sketched.

1. Introduction

Due to conceptual simplicity and display by averaging, subdivision surfaces are a popular representation for modeling, graphics and multiresolution (see e.g. [12], [5], [7], [17], [16], [8] and references therein). One of the noted drawbacks of subdivision surfaces for quantitative applications is their lack of a finite closed-form representation. Already the basic question, *what is the volume enclosed by a subdivision surface*, is not treated in the literature and does not seem to have a simple answer. Thus realistic animation – as opposed to cartoons – and geometric design using this convenient representation must rely on user intuition rather than computer guidance to generate objects that hold a given volume or, in the case of computing the center of mass, do not topple over. This gap in the subdivision arsenal is filled by the present paper. We develop an efficient and robust algorithm for measuring volumes of subdivision surfaces and sketch how higher-order moments can be treated in the same framework.

For comparison, consider first the direct approach of splitting the volume enclosed by the subdivision surface into tetrahedra or slices as is the common approach when measuring polyhedra [10],[1], [9]). The number of pieces to be measured for exact calculation is proportional to the number of facets. Since each polyhedron facet gives rise to a constant number of new facets with each subdivision step, the resulting amount of work is exponential in the number of subdivision steps and hence unpractical for real time applications. A more sophisticated approach is to compute the volume of the initial polyhedron and then track the change in volume due to the refinement, interpreting the refinement as a sequence of cuts applied to the solid enclosed by the polyhedron [13]. However, this tracking is not easily implemented since cuts, in general, are neither simple nor planar and may add or remove material depending on local convexity. The approach is also not efficient since the amount of work is still proportional to the exponential increase of the number of facets under subdivision.

Yet there is an efficient and robust approach to measuring the volume of most subdivision surfaces. Efficient means that the amount of work is constant at each subdivision step and robust means that a two-sided error bound exists and contracts by a constant multiple less than 1, typically 2^{-3}, with each refinement step.

The two key observations leading to the result are (1) that piecewise polynomial surfaces allow efficient computation of the exact volume and higher-order moments[6] and (2) that most popular subdivision schemes, e.g. [4],[2] [11], are modifications of box-spline subdivision rules, and hence generate a limit surface that is piecewise polynomial except at some isolated points, called extraordinary points. That is, while subdivision surfaces lack a global closed-form representation, increasing submeshes of the subdivision polyhedron have such a representation.

This said, the overall strategy is clear – namely to compute the asymptotic volume contributions exactly for the regular regions of the subdivision surface away from the extraordinary points, and to estimate and bound the volume contributions of the neighborhood of each extraordinary point.

For clarity we list our assumptions on the subdivision scheme.

† Supported by NSF Nationa Young Investigator grant 9457806-CCR

‡ Supported by an AUB grant

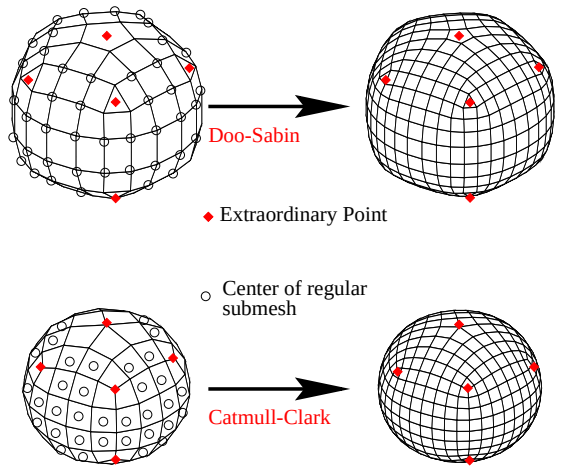

Figure 1: *Diamonds mark extraordinary points on the subdivision polyhedra. The centers of regular submeshes in the less refined polyhedra on the* left *are marked by circles. A regular submesh of the Doo-Sabin scheme (*top*) consists of four quadrilaterals surrounding a vertex. A regular submesh of the Catmull-Clark scheme (*bottom*) consists of eight quadrilaterals surrounding a quadrilateral.*

1. The subdivision scheme generates regular submeshes that refine to regular submeshes so that the number of extraordinary points remains constant.
2. Regular submeshes have a polynomial parametrization.
3. The subdivision algorithm has the local convex hull property. That is, new mesh points are convex combinations of old ones nearby, e.g. when the subdivision mask has only non-negative entries.

We proceed by showing, in Section 2, how the volume is computed by integrating over the surface, and compute the contribution of regular subsurfaces. Section 3 defines the approximation caps over the remaining volume and their integrals, and Section 4 gives a concrete example in terms of the Doo-Sabin subdivision. Section 5 outlines the computation of mass properties.

2. Volume contributions from regular submeshes

At each step, a subdivision algorithm creates a new mesh of points from an old mesh. A desirable property of any subdivision algorithm is that it generates increasing submeshes all of whose points have the same valence and whose facets all have the same number of edges. A submesh of points and facets with this standard valence and number of edges is called *regular*. Popular subdivision schemes derive their appeal from the fact that the limit surface is explicitly known for regular submeshes. For example, the limit surface of the Doo-Sabin subdivision scheme [4] applied to a regular nine-point submesh is a biquadratic tensor-product spline surface. The limit surface of the Catmull-Clark subdivision scheme [2] applied to a regular sixteen-point submesh is a bicubic tensor-product spline surface. And the limit surface of Loop's subdivision [11] is a linear combination of shifts of a 3-direction box spline. With respect to these subsurfaces we will apply Gauss' divergence theorem.

Given a parametrization

$$\mathbf{x}(\mathbf{u}) = [x,y,z](u,v) = \begin{pmatrix} x(u,v) \\ y(u,v) \\ z(u,v) \end{pmatrix}, \quad (u,v) \in U$$

of a surface S with normal

$$N = \mathbf{n}/|\mathbf{n}|, \quad \text{where} \quad \mathbf{n} = \frac{\partial \mathbf{x}}{\partial u} \wedge \frac{\partial \mathbf{x}}{\partial v}.$$

and given a map $\mathbf{f} : R^3 \mapsto R^3$, the divergence theorem (see e.g. [15] 10.51) states that

$$\int_V \nabla \cdot \mathbf{f}\, dV = \int_S \mathbf{f} \cdot N\, dS$$

i.e. that the integral of the divergence $\nabla \cdot \mathbf{f} = \sum \frac{\partial}{\partial x_i} f_i$ over the volume V equals the integral of the normal component $\mathbf{f} \cdot N = \sum f_i N_i$ over the surface S of V. By change of variable

$$\int_S dS = \int_U |\mathbf{n}|\, du dv$$

i.e. the area element $|\mathbf{n}|$ is the inverse of the normalization factor of the normal direction and hence

$$\begin{aligned} \int_V \nabla \cdot \mathbf{f}\, dV &= \int_S \mathbf{f} \cdot \mathbf{n}/|\mathbf{n}|\, dS \\ &= \int_U \mathbf{f} \cdot \mathbf{n}\, du dv. \end{aligned}$$

Now if both $\mathbf{f}$ and $\mathbf{x}$ are polynomial then the integrand is polynomial; and if U is a simple domain, say a triangle or square, then the integral can be determined efficiently, explicitly and exactly by averaging the Bernstein-Bézier coefficients [3]. If the parametrization $\mathbf{x}$ of S consists of patches $\mathbf{x}^i$ and U is the union of the patch domains U^i then

$$\int_U \mathbf{f} \cdot \mathbf{n}\, du dv = \sum_i \int_{U^i} \mathbf{f} \cdot \mathbf{n}^i\, du^i dv^i.$$

Choosing $\mathbf{f} = [0,0,z]$ we need only compute one component of $\mathbf{n}$,

$$n_3 = \frac{\partial x}{\partial u}\frac{\partial y}{\partial v} - \frac{\partial x}{\partial v}\frac{\partial y}{\partial u},$$

to determine the volume

$$\begin{aligned} \mathcal{V}_S := \int_V 1 dV &= \int_V \nabla \cdot [0,0,z] dV \\ &= \int_S [0,0,z] \cdot [n_1,n_2,n_3] dS \\ &= \int_U z\, n_3\, du dv. \end{aligned}$$

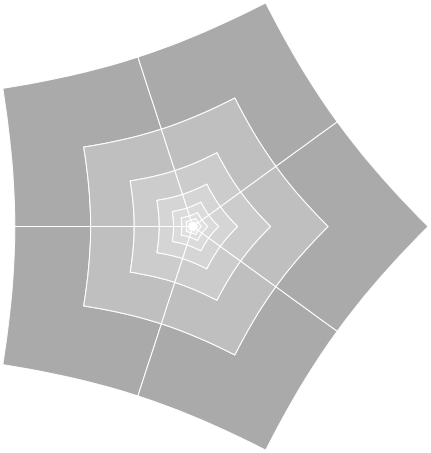

Figure 2: *Union of surface layers at a 5-valent extraordinary point.*

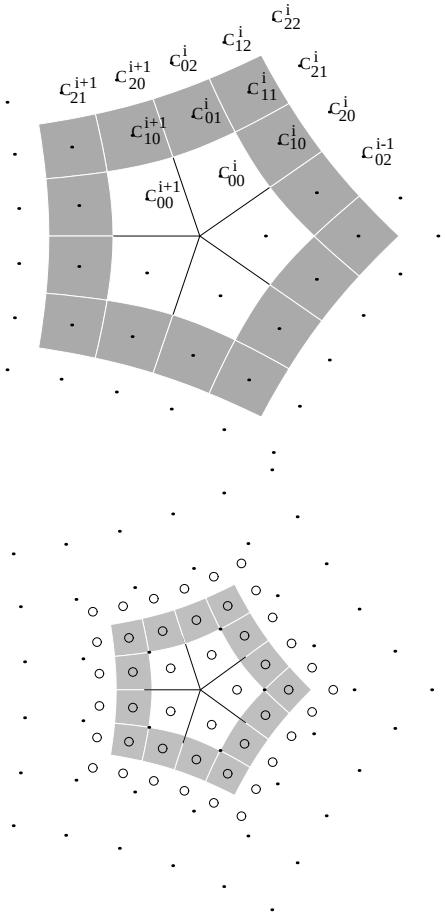

Figure 3: *On* top, *dots, some labelled C_{jk}^{i}, indicate the nodes of a submesh that determines the subdivision matrix at an extraordinary point in the Doo-Sabin scheme. The grey quadrilaterals each represent a biquadratic patch.* Below *circles indicate the nodes of the refined submesh. Again the biquadratic patches are delineated.*

The algorithm

Initially the algorithm computes the volume contribution V_0 for all, possibly zero, surface pieces corresponding to regular submeshes: for each patch (cf. Figure 3) $z(u,v)\cdot n_3(u,v)$ is computed and integrated. Each subsequent subdivision adds exactly one, geometrically ever smaller, layer of surface pieces defined by regular submeshes around each extraordinary point as shown in Figure 2 and Figure 3. Since the contributions to the volume by these regular layers are computed exactly and for the limit surface, the contribution of submeshes obtained by subdividing a regular submesh need not be recomputed! Thus the work at each subdivision step is constant, proportional only to the number of extraordinary points; in the mth step it consists of computing the surface integral V_m of the mth layer added at the extraordinary point. With W_m the surface integral of the cap whose construction is explained in Section 3, the approximation to the volume at the mth step is

$$\mathcal{V}_m = \sum_{i=0}^{m} V_i + W_m.$$

Section 4 gives a concrete example.

3. Volume contributions of the neighborhood of an extraordinary point

Having dealt with the regular parts of the mesh in the previous section, the goal of this section is to cap off the holes remaining in the regular surface around the extraordinary points and compute the integrals of the capping surfaces. To directly apply the divergence theorem, each cap should join the regular surface continuously and without gap or overlap.

Extraordinary points are typically either meshpoints with a valence different from the regular meshpoints, or centroids of mesh facets that have a different than the standard number of edges. For example, cf. Figure 1, the Doo-Sabin subdivision scheme has a standard valence of four for both vertices and facets, i.e. every mesh point is surrounded by four quadrilaterals.

The error bounding box

By assumption, the volume is bounded by the convex hull of the submesh in the neighborhood of the extraordinary point. Figure 3 schematically shows such a submesh for the Doo-Sabin scheme. The estimate can be improved by knot insertion, i.e. conversion to Bernstein-Bézier form at the boundary between the regular surface pieces and the neighborhood of the extraordinary point. Figure 4 shows the indices of the

Bernstein-Bézier coefficients b_{02}, b_{12}, b_{22}, b_{21}, b_{20} along the boundary for the Doo-Sabin subdivision. Since, depending on the valence of the extraordinary point, the exact convex hull may be expensive to compute, we settle for an efficiently computable bounding box that encloses the minimal and maximal values of each component of the control points in the neighborhood of the extraordinary point.

To get an estimate of the contraction of this error box it is natural and standard to look at the subdivision matrix which maps the submesh around the extraordinary point to a refined submesh with the same number of mesh points. For the Doo-Sabin scheme the matrix is of size $p \times p$ where $p = q \cdot 3 \cdot 3$ at a q-valent extraordinary point, e.g. $p = 45$ for the example in Figure 3. For a smooth-surfacing scheme the leading eigenvalue of this matrix is 1 and the two subdominant, next largest eigenvalues determine the first-order behavior of the subdivision surface and hence the asymptotic shrinkage factor of the submesh surrounding the extraordinary point [14]. Denoting the second-largest eigenvalue by $\lambda < 1$, the bounding box volume in three dimensions converges asymptotically on the order of λ^3 with each refinement step. In practical examples the asymptotic rate is immediately reached (c.f. Tables 1 and 2).

Finally we define the *caps*. To get a good estimate of the volume the cap patches must lie within the bounding box. We choose them as a ring, corresponding to the white quadrilaterals in Figure 4, of C^0-connected patches, of the same degree as the regular C^k subdivision surface, and extending the regular surface parametrically C^k to cover the neighborhood of the extraordinary point. This avoids gaps and determines $k+1$ layers of Bernstein-Bézier coefficients adjacent to the regular surface. Viewed as the result of knot insertion, the Bernstein-Bézier coefficients together with the coefficient or ring of coefficients closest to the extraordinary point form a convex hull of the limit surface. The remaining innermost ring(s) of coefficients may be determined by symmetry and knowledge of the limiting surface. – For example, for the Doo-Sabin algorithm, the C^1 extension determines all but the Bernstein-Bézier coefficient with index 00 (c.f. Figure 4). A natural choice for this coefficient is the centroid of the n-sided mesh cell which is interpolated by the limit surface. For the Catmull-Clark algorithm, the C^2 extension pins down all but one Bernstein-Bézier coefficient which we may choose to be the extraordinary point of the subdivision polyhedron.

4. Example: The volume of Doo-Sabin subdivision surfaces

The Doo-Sabin algorithm is a generalization of the subdivision scheme for biquadratic tensor product B-splines. For each n-gon of the original mesh, a new, smaller n-gon is created and connected with its neighbors as shown in Figure 5. The masks for generating a new n-gon from an old one are specified in Figure 6 for the regular case $n = 4$ *(left)*, and the general case *(right)*. In [4] Doo and Sabin suggest

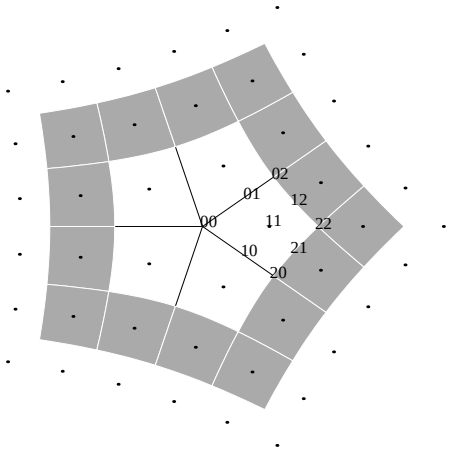

Figure 4: *Indices of the Bernstein-Bézier coefficients of a biquadratic extension.*

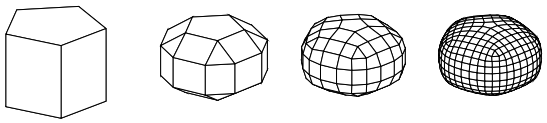

Figure 5: *Mesh refinement by the Doo-Sabin algorithm.*

$$\alpha^j = \frac{3+2\cos(2\pi j/n)}{4n} + \begin{cases} 1/4 & \text{if } j = 0 \\ 0 & \text{else} \end{cases}.$$

A regular Doo-Sabin submesh consists of nine points C_{ij} arranged as four quadrilateral facets surrounding a central point C_{11} (c.f. Figure 3):

$$\begin{array}{ccc} C_{02} & C_{12} & C_{22} \\ C_{01} & C_{11} & C_{21} \\ C_{00} & C_{10} & C_{20} \end{array}$$

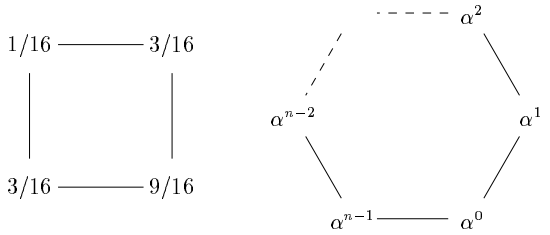

Figure 6: *Masks for the Doo-Sabin algorithm.*

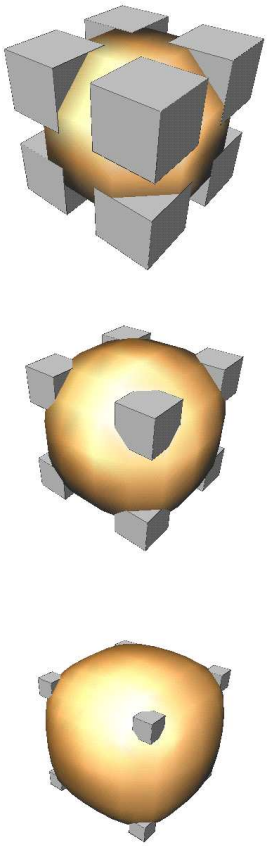

Figure 7: *Volume error boxes of the first three Doo-Sabin subdivisions of a cube-shaped mesh.*

subdivision	error box volume
1	5.27343e-02
2	1.04675e-02
3	1.04761e-03
4	1.16415e-04
5	1.36961e-05
6	1.66014e-06
7	2.04325e-07
8	2.53426e-08

Table 1: *Volume of each error box when subdividing the unit cube. The volume measured in the eighth subdivision is* 0.6291374278.

The points define a biquadratic patch with Bernstein-Bézier coefficients b_{jk} where

$$\begin{array}{lll} b_{02}=\frac{1}{4}\begin{pmatrix}C_{02}+C_{12}\\+C_{01}+C_{11}\end{pmatrix} & b_{12}=\frac{1}{2}\begin{pmatrix}C_{02}\\+C_{12}\end{pmatrix} & b_{22}=\frac{1}{4}\begin{pmatrix}C_{22}+C_{12}\\+C_{21}+C_{11}\end{pmatrix} \\ b_{01}=\frac{1}{2}\begin{pmatrix}C_{01}+C_{11}\end{pmatrix} & b_{11}=C_{11} & b_{21}=\frac{1}{2}\begin{pmatrix}C_{21}+C_{11}\end{pmatrix} \\ b_{00}=\frac{1}{4}\begin{pmatrix}C_{01}+C_{00}\\+C_{10}+C_{11}\end{pmatrix} & b_{10}=\frac{1}{2}\begin{pmatrix}C_{10}\\+C_{11}\end{pmatrix} & b_{20}=\frac{1}{4}\begin{pmatrix}C_{20}+C_{21}\\+C_{10}+C_{11}\end{pmatrix} \end{array}$$

For this patch, $z\,n_3$ is a scalar-valued biquintic polynomial. Denoting its Bernstein-Bézier coefficients by p_{ij} its integral is $\frac{1}{36}\sum_{i=0}^{5}\sum_{j=0}^{5}p_{ij}$.

To cap the neighborhood of the extraordinary point for the given subdivision step, the coefficients C^i_{jk} generate the Bernstein-Bézier coefficients of a ring of biquadratic patches defined by C^1 extension and interpolation of the centroid:

$$\begin{aligned} b^i_{02} &= \frac{1}{4}(C^i_{00}+C^i_{01}+C^{i+1}_{00}+C^{i+1}_{10}) \\ b^i_{12} &= \frac{1}{2}(C^i_{00}+C^i_{01}) \\ b^i_{22} &= \frac{1}{4}(C^i_{00}+C^i_{01}+C^i_{10}+C^i_{11}) \\ b^i_{01} &= \frac{1}{2}(C^i_{00}+C^{i+1}_{00}) \\ b^i_{11} &= C^i_{00} \\ b^i_{21} &= \frac{1}{2}(C^i_{00}+C^i_{10}) \\ b^i_{00} &= \frac{1}{n}\sum_{i=1}^{n}C^i_{00} \\ b^i_{10} &= \frac{1}{2}(C^i_{00}+C^{i-1}_{00}) \\ b^i_{20} &= \frac{1}{4}(C^i_{00}+C^i_{10}+C^{i-1}_{00}+C^{i-1}_{01}). \end{aligned}$$

The subdominant eigenvalue of the subdivision matrix is $\lambda = 1/2$ implying an asymptotic reduction of the error box volume by 2^{-3}. Indeed, the error bounds are confirmed by Table 1 and Table 2 with a graphical interpretation shown in Figure 4 and Figure 8. A tighter error bound could be obtained by observing that $C^i_{00} = b^i_{11}$ implies that the limit surface lies in the convex hull of the Bernstein-Bézier coefficients of the cap.

5. Extension to higher-order Moments

The procedure outlined for the zeroth order moment, the volume, is easily extended to higher-order moments (c.f. [6]). For example, to compute the x-component of the center of mass we can choose $\mathbf{f} = [0, 0, xz]$. As a visual aid a mass error-box whose size is the sum of the individual error boxes may be placed at the center of mass of the approximate surface.

References

1. BERNARDINI, F. Integration of polynomials over n-dimensional polyhedra. *Computer Aided Design 23(1)* (1991), 51–58.

2. CATMULL, E., AND CLARK, J. Recursively generated B-spline surfaces on arbitrary topological meshes. *Computer Aided Des. 10* (1978), 350 – 355.

3. DE BOOR, C. B-form basics. In *Geometric Modeling: Algorithms and New Trends*, G. Farin, Ed. SIAM, Philadelphia, 1987, pp. 131–148.

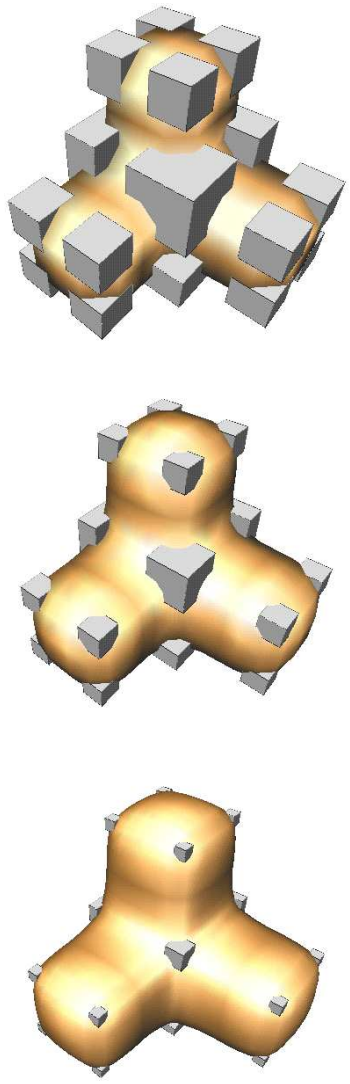

Figure 8: *Volume error boxes for a stencil shape.*

valence	subdivision 1	2	3
3	0.052734	0.010467	0.001047
4	0.125797	0.034572	0.004076
5	0.143717	0.033833	0.003127
6	0.264948	0.066169	0.006275

Table 2: *Volume of error boxes for extraordinary points of valence 3,4,5,6 when subdividing the stencil shape.*

4. DOO, D., AND SABIN, M. Behaviour of recursive subdivision surfaces near extraordinary points. *Computer Aided Des. 10*, 6 (Nov 1978), 356–360.

5. DYN, N., LEVIN, D., AND GREGORY, J. A. A butterfly subdivision scheme for surface interpolation with tension control. *ACM Trans. on Graphics 9* (1990), 160 – 169.

6. GONZALEZ-OCHOA, C., MCCAMMON, S., AND PETERS, J. Computing moments of piecewise polynomial surfaces. *xxx xx* (199x). submitted.

7. HOPPE, H., DEROSE, T., DUCHAMP, T., HALSTEAD, M., JIN, H., MCDONALD, J., SCHWEITZER, J., AND STUETZLE, W. Piecewise smooth surface reconstruction. *Computer Graphics – Proceedings of Siggraph 94* (1994), 295–302.

8. KOBBELT, L. Interpolatory subdivision on open quadrilateral nets with arbitrary topology. vol. 15, Basil Blackwell Ltd. Eurographics 96 conference issue.

9. LEE, Y. T., AND REQUICHA, A. A. G. Algorithms for computing the volume and other integral properties of solids. II a family of algorithms based on representation conversion and cellular approximation. *Commun. ACM (USA) 25* (Sept. 1982), 642–650.

10. LIEN, S., AND KAJIYA, J. A symbolic method for calculating the integral properties of arbitrary nonconvex polyhedra. *IEEE Computer Graphics and Applications 4(9)* (Oct 1984), 35–41.

11. LOOP, C. Smooth subdivision for surfaces based on triangles. *Thesis, Univ. of Utah* (1987).

12. NASRI, A. Polyhedral subdivision methods for free-form surfaces. *ACM Transactions on Graphics 6* (1987), 29–73.

13. NASRI, A. An algorithm to compute volume of solids defined by recursive subdivision surfaces. Tech. rep., American University of Beirut, 1996. TR-96-01.

14. REIF, U. A unified approach to subdivision algorithms near extraordinary vertices. *CAGD 12* (1995), 153–174.

15. RUDIN, W. *Real and complex analysis*. Series in Higher Mathematics. McGraw-Hill, 1987.

16. SCHRODER, SWELDENS, AND ZORIN. Interpolating subdivision for meshes with arbitrary topology. *Computer Graphics – Proceedings of Siggraph 96* (1996), 189–192.

17. STOLLNITZ, E. J., DEROSE, T. D., AND SALESIN, D. H. *Wavelets for computer graphics: theory and applications*. Morgan Kaufmann, San Francisco, Calif, 1996.